



Monovacant polyoxometalates incorporated into MIL-101(Cr): novel heterogeneous catalysts for liquid phase oxidation



Carlos M. Granadeiro^a, André D.S. Barbosa^a, Patrícia Silva^b, Filipe A. Almeida Paz^b, Vipin K. Saini^c, João Pires^c, Baltazar de Castro^a, Salette S. Balula^{a,*}, Luís Cunha-Silva^{a,*}

^a REQUIMTE & Department of Chemistry and Biochemistry, Faculty of Sciences, University of Porto, 4169-007 Porto, Portugal

^b Department of Chemistry, CICECO, University of Aveiro, 3810-193 Aveiro, Portugal

^c Departamento de Química e Bioquímica, CQB, Faculdade de Ciências, Universidade de Lisboa, Campo Grande C8, 1749-016 Lisboa, Portugal

ARTICLE INFO

Article history:

Received 20 September 2012

Received in revised form

24 November 2012

Accepted 17 December 2012

Available online 4 January 2013

Keywords:

Polyoxometalates

Metal organic-framework

Hybrid materials

Heterogeneous catalysis

Oxidation

ABSTRACT

Two novel hybrid composite materials, $PW_{11}@MIL-101$ and $SiW_{11}@MIL-101$, were prepared by the inclusion of the potassium salts of the monovacant polyoxotungstates, $[PW_{11}O_{39}]^{7-}$ (PW_{11}) and $[SiW_{11}O_{39}]^{8-}$ (SiW_{11}), into the porous Metal–Organic Framework MIL-101(Cr). Materials were characterized by a myriad of solid-state methods such as powder X-ray diffraction (XRD), vibrational (FT-IR and FT-Raman) and ^{31}P solid-state NMR spectroscopies, elemental analysis, scanning electron microscopy (SEM) and energy-dispersive X-ray spectroscopy (EDX), and textual analysis confirming the incorporation of the POMs into MIL-101(Cr). $PW_{11}@MIL-101$ and $SiW_{11}@MIL-101$ revealed to be active, selective and recyclable catalysts for the oxidation of cis-cyclooctene, geraniol and R-(+)-limonene using the H_2O_2 as oxidant. Only one product was obtained from the epoxidation of cis-cyclooctene and geraniol: 1,2-epoxycyclooctane and 2,3-epoxygeraniol, respectively. In the oxidation of R-(+)-limonene the main products were limonene-1,2-epoxide and limonene-1,2-diol, however the diepoxide was also formed. Both composite materials, $PW_{11}@MIL-101$ and $SiW_{11}@MIL-101$, are recyclable for, at least, three consecutive cycles without significant loss of activity. The stability of the composites after the catalytic cycles was confirmed by several techniques. Remarkably, the MOF framework was found to play an important role in the stability of the PW_{11} in the presence of H_2O_2 .

© 2013 Elsevier B.V. All rights reserved.

1. Introduction

Metal–Organic Frameworks (MOFs), also known as coordination polymers, are nowadays on top of research in materials chemistry. In the last decade an extraordinary progress on the investigation and development of MOFs has been noticed, yielding novel functional materials with remarkable potential for gas storage, separation [1–5] and catalysis [6–10]. The success of these hybrid framework-based materials comes from the diversity of metal or metallic clusters that are interconnected with various functionalized organic linkers, often leading to tri-dimensional (3D) porous structures with large, regular and accessible cages and tunnels. According with their porous morphology, their cavities may act as nano-reactors because they can accommodate catalytically active molecules with adequate shape and size to enter the pores. The possibility of the inclusion depends on the correlation between their size and the accessible dimensions of the windows of each

cage. Furthermore, the large cavities of certain MOFs can promote a concentration effect between the different components from the catalytic reaction (catalysts, substrate and others), which may be required to improve yields and reduce reaction time. Heterogeneous catalysis using MOFs is, however, a relatively recent subject that needs to be explored. Recently, the 3D porous MOF material MIL-101(Cr) has shown to have important capacities for catalyst engineering [11–15]. This hybrid material originally prepared by Férey et al. is one of the most promising porous MOF discovered to date [16–18]. In fact, MIL-101(Cr) allows the introduction of nanoparticles, large molecular inorganic species and drugs within its cages [16,19,20].

The opportunity of incorporating Keggin-type polyoxometalates (POMs) in porous MOFs arises as an attractive pathway to exploit the catalytic activity of these species and opens the opportunity to create new catalytic systems that transform cheap natural compounds into valuable products. Keggin-type POMs are economical and environmentally attractive catalysts for oxidation reactions, both in laboratorial and industrial processes [21]. During the last decades, POMs have been studied as effective homogeneous catalysts in the oxidation of several hydrocarbons with H_2O_2 [21–28]. More recently much work is focussed in the

* Corresponding authors. Tel.: +351 220402576; fax: +351 220402659.

E-mail addresses: sbalula@fc.up.pt (S.S. Balula), l.cunha.silva@fc.up.pt (L. Cunha-Silva).

immobilization of POMs due to the necessity of recovering and recycling these active catalytic compounds. Different methodologies have been studied using various solid supports to immobilize POMs via dative, covalent or electrostatic binding [29–36]. The immobilization of POMs into nanoporous MIL-101(Cr) was performed only few years ago and the first studies using these composites as heterogeneous catalysts were only performed very recently. To date, Kholdeeva et al. have been using POMs@MIL-101 as catalysts for oxidative reactions, using titanium, cobalt monosubstituted phosphotungstates and the Keggin anion $[\text{PW}_{12}\text{O}_{40}]^{3-}$ as active catalyst centres, with O_2 and H_2O_2 being used as oxidants [13,31,37,38]. Kapteijn et al. reported the use of POMs@MIL-101, using the $\text{H}_3[\text{PW}_{12}\text{O}_{40}]$ in reactions of condensation, esterification, oxidation and hydrogenation [39,40]. Furthermore, the inclusion of $\text{H}_3[\text{PW}_{12}\text{O}_{40}]$ in other 3D porous MOF (Cu-btc) to prepare active heterogeneous catalysts has been also recently investigated [41–44].

In contrast with the monosubstituted POMs, the catalytic activity of monovacant POMs is not extensively explored. Furthermore, the immobilization studies performed with monovacant POMs are particularly scarce and only a couple of studies describe them as catalysts for oxidation reactions [34–36,45–47]. The present investigation reports the notable catalytic activity of the monovacant phosphotungstate ($[\text{PW}_{11}\text{O}_{39}]^{7-}$) and silicotungstate ($[\text{SiW}_{11}\text{O}_{39}]^{8-}$) anions incorporated into the MIL-101(Cr) cavities for the oxidations of alkenes and allylic alcohols using H_2O_2 as oxidant. This is one of the most attractive oxidant because it is fairly inexpensive and easily handled. The robustness and the recyclability of the composites were confirmed and the presence of monovacant POMs seemed to promote the stability of these hybrid materials under oxidative environment.

2. Experimental

2.1. Materials and methods

All reagents used in the preparation of the support material, namely chromium(III) nitrate nonahydrate $[\text{Cr}(\text{NO}_3)_3 \cdot 9\text{H}_2\text{O}]$, Aldrich, 99%, benzene-1,4-dicarboxylic acid ($\text{C}_8\text{H}_6\text{O}_2$, Aldrich, 98%) and hydrofluoric acid (HF, Aldrich, 40–45%) were used as received. Geraniol ($\text{C}_{10}\text{H}_{18}\text{O}$, Aldrich, 98%), cis-cyclooctene (C_8H_{14} , Aldrich, 95%) and R-(+)-limonene ($\text{C}_{10}\text{H}_{16}$, Aldrich, 97%) were purchased from commercial suppliers and used without further purification, as well as acetonitrile (CH_3CN , Panreac, 99%), hydrogen peroxide (H_2O_2 , Riedel de-Häen or Aldrich, 30%), ceric sulphate $[\text{Ce}(\text{SO}_4)_2]$, Aldrich, 99%.

Elemental analysis for Cr, P, Si and W were performed by ICP spectrometry (University of Santiago de Compostela, CACTUS-LUGO).

Electronic absorption spectra were recorded on Varian Cary 50 Bio spectrophotometer.

Infrared absorption spectra were obtained on a Jasco 460 Plus spectrometer, using KBr pellets. FT-Raman spectra were recorded on a RFS-100 Bruker FT-spectrometer, equipped with a Nd:YAG laser with excitation wavelength of 1064 nm, with laser power set to 350 mW.

Nitrogen (Air Liquide, 99.999%) physisorption experiments were made at -196°C using a volumetric apparatus (NOVA 2200e, surface area and pore size analyzer). For every experiment, about 20 mg of sample was degassed for 2.5 h at 120°C at low pressure ($<0.133\text{ Pa}$). The pore size distribution (PSD) curves were obtained by the BdB-FHH method. Micropore volumes V_{μ} , were obtained from t -plots, using an appropriate non-porous reference material. The total pore volume V_{total} , was estimated by the amount adsorbed at $p/p^0 \approx 0.95$.

Powder X-ray diffraction analyses were collected at ambient temperature on a X'Pert MPD Philips diffractometer, equipped with an X'Celerator detector and a flat-plate sample holder in a Bragg-Brentano para-focusing optics configuration (45 kV, 40 mA). Intensity data were collected by the step-counting method (step 0.04°), in continuous mode and, in the $ca. 3.5 \leq 2\theta \leq 50^\circ$ range.

Solid-state ^{31}P HPDEC NMR spectra were recorded on a 9.4 T Bruker Avance 400 spectrometer (HPDEC stands for high-power decoupled).

Scanning electron microscopy (SEM) images were performed in a high resolution scanning electron microscope Hitachi SU-70 instrument working at 4 kV. The energy-dispersive X-ray spectroscopy (EDX) studies and SEM mapping images were recorded in the same microscope working at 15 kV and using a Bruker QUANTAX 400 EDS microanalysis system. Samples were analyzed as powders and prepared by deposition on aluminium sample holders followed by carbon coating using a Emitech K950X carbon evaporator.

GC-MS analyses were performed using a Hewlett Packard 5890 chromatograph equipped with a Mass Selective Detector MSD series II using helium as the carrier gas (35 cm s^{-1}); GC-FID was performed using a Varian CP-3380 chromatographer to monitor the homogeneous reactions and heterogeneous reactions. The hydrogen was the carrier gas (55 cm s^{-1}) and fused silica Supelco capillary columns SPB-5 ($30\text{ m} \times 0.25\text{ mm i.d.}$; $25\text{ }\mu\text{m}$ film thickness) were used.

2.2. Synthesis and preparation of materials

Monovacant polyoxotungstates. The potassium and tetrabutylammonium (TBA) salts of monovacant $[\text{PW}_{11}\text{O}_{39}]^{7-}$ and $[\text{SiW}_{11}\text{O}_{39}]^{8-}$: $\text{K}_7[\text{PW}_{11}\text{O}_{39}] \cdot 10\text{H}_2\text{O}$ (KPW₁₁), $\text{K}_8[\text{SiW}_{11}\text{O}_{39}] \cdot 13\text{H}_2\text{O}$ (KSiW₁₁), $\text{TBA}_4\text{H}_3[\text{PW}_{11}\text{O}_{39}]$ (PW₁₁), $\text{TBA}_4\text{H}_4[\text{SiW}_{11}\text{O}_{39}]$ (SiW₁₁), were prepared using reported procedures [28,48–50]. All these polyoxotungstates were characterized by elemental and thermal analysis, FT-IR and FT-Raman spectroscopy, NMR spectroscopy and powder XRD, confirming the synthesis of the desired compounds.

Solid support MIL-101 (Cr). The porous metal-organic framework (MOF) material MIL-101(Cr) was prepared by an adaptation of the method described by Férey et al. [16]. A mixture containing chromium(III) nitrate (2 mmol), benzene-1,4-dicarboxylic acid (2 mmol) and hydrofluoric acid (100 μL) in 10 mL of H_2O was stirred at room temperature to obtain an homogeneous suspension, transferred into an autoclave and heated at 493 K for 9 h in an electric oven. After a slowly cooling process (inside the oven), the material was isolated by filtration and purified through a double DMF treatment and a double ethanol treatment. Selected FT-IR (cm^{-1}): 3440, 2933, 1671, 1625, 1508, 1405, 1385, 1017, 748, 663, 590; selected FT-Raman (cm^{-1}): 3077, 2929, 1613, 1496, 1459, 1146, 1044, 872, 812, 632.

Composite materials XW₁₁@MIL-101. The composite materials were prepared through the immobilization of the potassium salts of monovacant polyoxotungstates (KPW₁₁ and KSiW₁₁) in the porous solid support MIL-101(Cr) using a modified procedure of the method described by Maksimchuk et al. [37]. Briefly, aqueous solutions of KPW₁₁ and KSiW₁₁ (10 mM; 50 mL) were added to the MIL-101(Cr) (0.5 g) and stirred at room temperature for 24 h. The solid was filtrated, washed thoroughly with water and dried in a dessicator over silica gel.

PW₁₁@MIL-101. Anal. found (%): Cr, 10.2; W, 12.9; P, 1.20; loading of PW₁₁: 0.066 mmol per 1 g. Selected FT-IR (cm^{-1}): 3466, 2925, 1623, 1556, 1508, 1403, 1043, 1018, 952, 886, 830, 814, 748, 673, 663. Selected FT-Raman (cm^{-1}): 3073, 2933, 1613, 1493, 1457, 1145, 1028, 1001, 974, 871, 811, 785, 632.

SiW₁₁@MIL-101. Anal. found (%): Cr, 10.2; W, 13.3; Si, 1.34; loading of SiW₁₁: 0.073 mmol per 1 g. Selected FT-IR (cm^{-1}): 3429, 2925,

1711, 1682, 1621, 1554, 1398, 1021, 910, 811, 746, 553. Selected FT-Raman (cm^{-1}): 3080, 2924, 1613, 1493, 1458, 1145, 1028, 976, 959, 872, 811, 785, 632.

2.3. Catalytic studies

The oxidation reactions of *cis*-cyclooctene (i), geraniol (iii) and *R*-(+)-limonene (v) (Scheme 1) were carried out in acetonitrile (MeCN), using a borosilicate 10 mL reaction vessel, with addition of H_2O_2 (30 wt.%), in the presence of the monovacant polyoxometalates (PW_{11} and SiW_{11}) as homogeneous catalysts and the respective composite materials (PW_{11} @MIL-101 and SiW_{11} @MIL-101) as heterogeneous catalysts. In the oxidation of geraniol the reaction was performed at room temperature and protected from light. The oxidative reactions of *cis*-cyclooctene and *R*-(+)-limonene were carried out at 75 °C. In a typical experiment, the substrate (1 mmol) and the catalyst (3 μmol), placed in the reaction vessel, were dissolved in MeCN (1.5 ml) and stirred. The H_2O_2 was added to the reaction mixture, 500 μL (4.5 mmol) for the oxidation of geraniol and *R*-(+)-limonene and 105 μL (1 mmol) for the oxidation of *cis*-cyclooctene. The reactions were followed by GC analysis and stopped when a complete conversion of the substrate was observed or when the product yields remained constant after two successive GC analyses. At regular intervals, an aliquot was taken directly from the reaction mixture with a microsyringe (approximately 10 μL), diluted in MeCN, centrifuged and injected into the GC or GC–MS equipment for analysis of starting materials and products. Each experiment was reproduced at least twice. The maximum error obtained between repeated experiments for the conversion data of each substrate was never higher than 5% for the oxidation of *cis*-cyclooctene, 9% for the oxidation of geraniol and 8% for the oxidation of *R*-(+)-limonene. The reaction products reported were identified as described elsewhere [51,52]. In the presence of monovacant composites (42 mg of PW_{11} @MIL-101 and 46 mg of SiW_{11} @MIL-101), the heterogeneous catalysts were centrifuged at the end of reactions, washed with MeCN several times to remove the remaining substrate, reaction products and oxidant. The recovered catalyst was dried at room temperature overnight and reused in a new reaction under identical experimental conditions, with readjustment of all quantities, without changing the molar ratios and reaction concentrations. After the consecutive reaction cycles, the monovacant composites were analyzed by different techniques as well as by tungsten analysis. Blank reactions were performed for all substrates, confirming that no oxidation products are obtained unless the catalyst and H_2O_2 are present. Even in the presence of the support MIL-101(Cr) substrates conversion was not higher than 10% after 24 h of reaction.

2.4. Titration of hydrogen peroxide

At the end of each heterogeneous catalytic reaction, an aliquot was taken from the reaction mixture for the determination of hydrogen peroxide in solution. The sample without solid catalyst was accurately weighed, quickly dissolved in diluted sulphuric acid and the peroxides titrated against 0.1 N ceric sulphate, using ferroin as indicator [53].

3. Results and discussion

3.1. Composite materials preparation and characterization

The preparation of the composite materials (PW_{11} @MIL-101 and SiW_{11} @MIL-101) was carried out by immobilization through impregnation of potassium salts of the monovacant polyoxotungstates (KPW_{11} and KSiW_{11} , respectively) in the porous MIL-101(Cr) in aqueous solution. The prospective inclusion of the

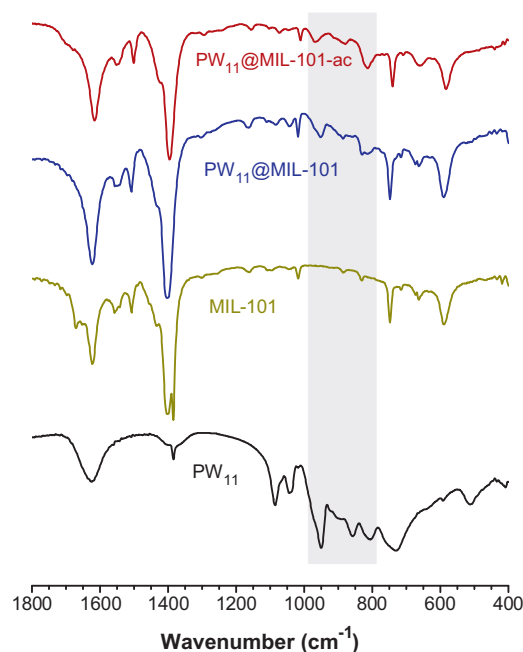
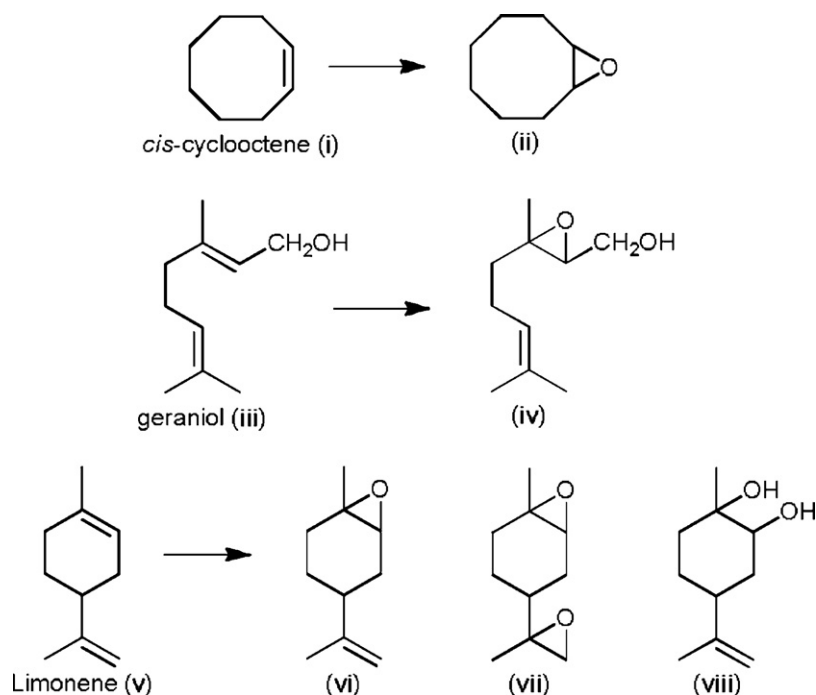


Fig. 1. FT-IR spectra of PW_{11} , the solid support MIL-101(Cr), and the composite material before (PW_{11} @MIL-101) and after catalysis (PW_{11} @MIL-101-ac), shown between 1800 and 400 cm^{-1} . (For interpretation of the references to colour in this figure legend, the reader is referred to the web version of this article.)

PW_{11} and SiW_{11} in support material MIL-101(Cr) was monitored by UV/Vis spectroscopy. As depicted in Fig. S1 (see the Supporting Information), the decrease of the absorbance of the band at ca. 250 nm (assigned to the charge transition from the bridging O-atoms to W-atoms) for their respective solutions after 24 h of reaction relatively to the correspondent initial polyoxotungstate solutions, supports the reduction of the amount of POMs. This reduction strongly suggests the incorporation of the POMs (PW_{11} and SiW_{11}) in the MIL-101(Cr) framework, leading to the composite materials. Indeed, the utilization of a myriad of characterization methods, such as powder XRD, vibrational (FT-IR and FT-Raman) and ^{31}P HPDEC NMR spectroscopies, elemental analysis (ICP), scanning electron microscopy (SEM) and energy-dispersive X-ray spectroscopy (EDX) and textural analysis (N_2 adsorption isotherms and pore size distribution), further support the preparation of PW_{11} @MIL-101 and SiW_{11} @MIL-101.

The presence of the polyoxotungstates in the MIL-101(Cr) framework was initially established by FT-IR and FT-Raman spectroscopic studies of the composite materials in comparison with the isolated compounds. The FT-IR spectra of both composite materials exhibit the typical bands of the MOF as well as some of the vibrational modes of the POMs (Fig. 1 and Fig. S2-left of the Supporting Information for the PW_{11} and SiW_{11} based materials, respectively). Regarding the PW_{11} @MIL-101 material, the infrared spectrum shows bands located at 1043, 952 and 814 cm^{-1} assigned to the P–O, W=O and W–O–W stretching modes of the phosphotungstate, respectively (Fig. 1) [54].

Similarly, the spectrum of the composite SiW_{11} @MIL-101 exhibits bands at approximately 1021, 910 and 811 cm^{-1} that correspond to Si–O, W=O and W–O–W stretches of the silicotungstate, respectively (see Fig. S2-left of the Supporting Information) [54]. The FT-Raman spectra of the composite materials further support the inclusion of the polyoxotungstates into the MIL-101(Cr) cavities. Besides the characteristic bands of MIL-101(Cr), the spectra also exhibit new small bands located at approximately 1028 and 975 cm^{-1} assigned to M–O and W=O stretching modes, respectively (see Fig. 2 for PW_{11} @MIL-101 and



Scheme 1. Chemical structure of the substrates investigated and their respective oxidation products.

Fig. S2-right of the Supporting Information for SiW₁₁@MIL-101) [54].

The formation of the PW₁₁@MIL-101 composite and the structural stability of the PW₁₁ after inclusion in the MIL-101(Cr) material are also supported by ³¹P solid-state NMR spectroscopy. The ³¹P HPDEC MAS NMR spectra of the PW₁₁

and composite material PW₁₁@MIL-101 are compared in Fig. 3. Indeed, the single peak observed at –10.70 ppm in the PW₁₁ spectrum, unequivocally attributed to the [PW₁₁O₃₉]⁷⁻ anion as confirmed by various literature reports [16,50,55,56], is

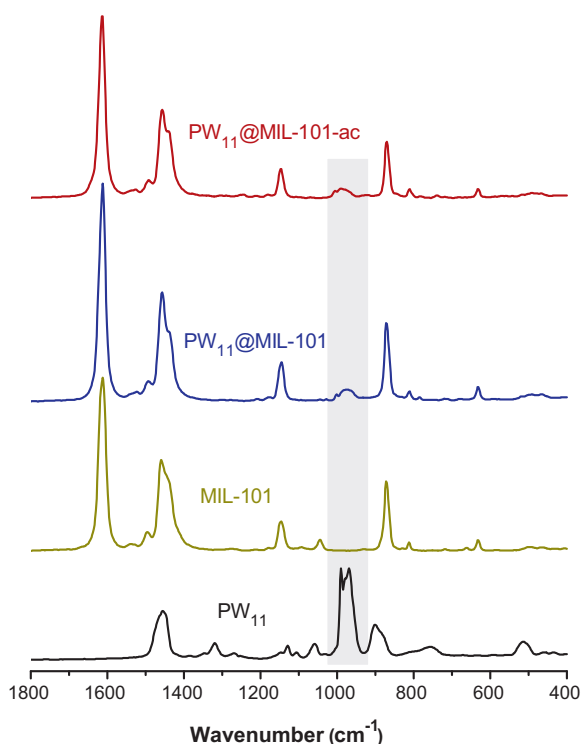


Fig. 2. FT-Raman spectra of PW₁₁, the solid support MIL-101(Cr), and the composite material before (PW₁₁@MIL-101) and after catalysis (PW₁₁@MIL-101-ac), depicted in the wavenumber range of 1800–400 cm⁻¹. (For interpretation of the references to colour in this figure legend, the reader is referred to the web version of this article.)

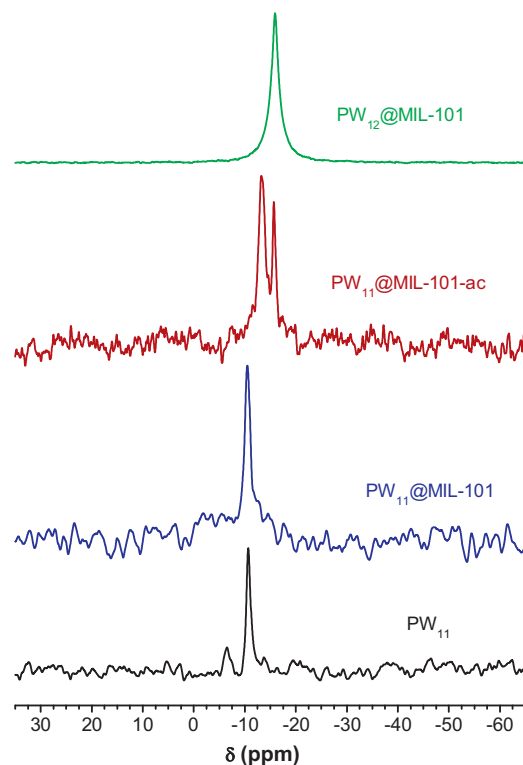


Fig. 3. ³¹P HPDEC MAS spectra of the PW₁₁, and the PW₁₁ based composite material before (PW₁₁@MIL-101) and after catalysis (PW₁₁@MIL-101-ac), and the composite PW₁₂@MIL-101, shown in the chemical shift range of –65 to 35 ppm. (For interpretation of the references to colour in this figure legend, the reader is referred to the web version of this article.)

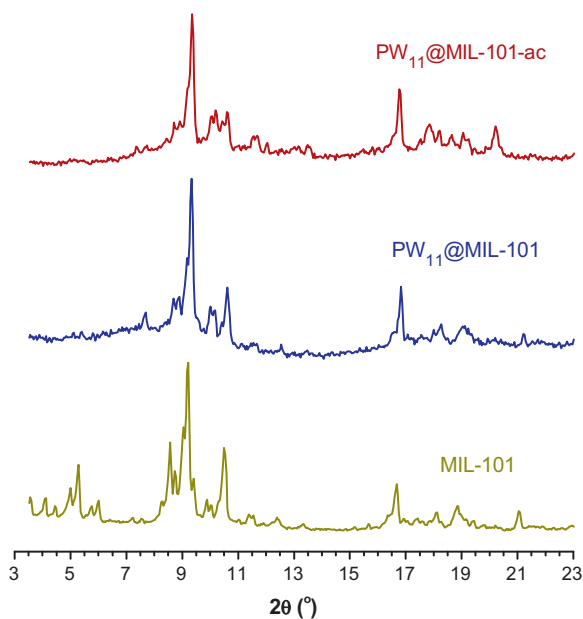


Fig. 4. Powder XRD patterns of the solid support MIL-101(Cr), and the PW_{11} -based composite material before ($PW_{11}@MIL-101$) and after catalysis ($PW_{11}@MIL-101-ac$).

also found in the $PW_{11}@MIL-101$ spectra ($\delta = -10.65$ ppm). This indicates that the structure of the monovacant PW_{11} is retained after its inclusion in MIL-101 cages as previously verified for other composite materials of this monovacant POM [35,45,57].

The powder XRD patterns of the composite materials, $PW_{11}@MIL-101$ and $SiW_{11}@MIL-101$, indicates that the crystalline structure of the porous MIL-101(Cr) is maintained after the inclusion of the polyoxotungstates, as their main diffraction peaks remained practically unaffected (see Fig. 4 and Fig. S3 of the Supporting Information, for the PW_{11} and SiW_{11} based materials, respectively). Furthermore, the crystalline phases (packing arrangement) of PW_{11} and SiW_{11} are totally modified in the course of their insertion into the solid support, since diffraction peaks of these polyoxotungstates are not noticeable in the diffraction patterns of the respective composite material. This piece of evidence confirms that both the PW_{11} and SiW_{11} complexes present in the materials are in non-crystalline form, presumably as consequence of their inclusion and dispersion in the solid support cavities.

The maintenance of the crystalline structure of the solid support after the incorporation of PW_{11} or SiW_{11} was also confirmed by electron microscopy (SEM and EDX). As depicted in Fig. 5, the SEM images of $PW_{11}@MIL-101$ (Fig. 5b) and $SiW_{11}@MIL-101$ (Fig. 5d) composite materials reveal cubic micro-crystals with identical morphology (size and shape) of those of the solid support MIL-101(Cr) (Fig. 5a), pointing to the preservation of the structure of the MIL-101(Cr) in the composite materials. EDX spectra (not shown) reveal the presence of P and W, or Si and W, in the respective materials $PW_{11}@MIL-101$ and $SiW_{11}@MIL-101$. Furthermore, the EDX elemental mapping images show a uniform distribution of P and W (from PW_{11}), and Cr and O (from MIL-101(Cr))—see Fig. S4 of the Supporting Information) confirming a homogenous dispersion of the PW_{11} in the MIL-101(Cr) framework, most probably placed inside the cavities of the porous support material (Fig. 6a). Identical results were observed in the EDX mapping analysis of the other composite material, $SiW_{11}@MIL-101$ (see Fig. S5 of the Supporting Information).

The nitrogen adsorption–desorption isotherms of MIL-101(Cr), and POMs incorporated MIL-101(Cr) samples are presented in Fig. 7. The shape of these samples is predominantly type I, with

Table 1

Textural properties of MIL-101(Cr), composite materials and their respective samples after catalysis (ac).

	A_{BET} (m ² /g)	V_{μ} (cm ³ /g)	V_{total} (cm ³ /g)
MIL-101(Cr)	2846	1.17	1.30
$PW_{11}@MIL-101$	1720	0.74	0.80
$PW_{11}@MIL-101-ac$	1324	0.56	0.63
$SiW_{11}@MIL-101$	1795	0.76	0.87
$SiW_{11}@MIL-101-ac$	1611	0.68	0.80

slight type IV features [58]. This result is in line with the type of porosity described for MIL-101(Cr) [59] and total adsorbed amounts also agree with data previously published in the literature [16]. Materials show polymodal pore size distribution (see Fig. S6 of the Supporting Information). The textural properties of these materials, in particular the BET surface area, microporous volume (V_{μ}) and total pore volume V_{total} are listed in Table 1. The incorporation of PW_{11} and SiW_{11} into the MIL-101(Cr) framework is apparent here, as it leads to reduction of 40% and 37% in surface area, respectively (Table 1). Likewise, it also leads to the 38% and 33% reduction in total pore volume, respectively. Elemental analysis results indicate a POM loading of 20% and 21% for the $PW_{11}@MIL-101$ and $SiW_{11}@MIL-101$ composites, respectively. As previously described by Férey et al. we have assumed that the POMs, due to their size, could only be present in the large cavities of MIL-101(Cr). We have estimated the presence of approximately 4 monovacant Keggin-type units per cavity in both composites.

Pore Size Distribution (PSD) gets altered upon incorporation of POMs (see Fig. S6 of the Supporting Information). In MIL-101(Cr) the majority of pores are of 2.4 and 3.0 nm sizes and both sizes are in comparable amounts. But after incorporation of POMs, either PW_{11} or SiW_{11} , the PSD band for small pores is shifted to a broader PSD between 2.4 and 2.7 nm, on the other hand, the PSD band for larger pores get shifted around 3.3 nm. These observations indicate that smaller pore (with pore window 1.2 nm) [59] could have difficulty in sufficient loading of POMs units (size ~ 1.0 nm) that is comparable to pore window [60]. It also suggests that larger pores with eventually larger pore window (1.6 nm) have received most of the POMs loading selectively. Therefore, the broadening of smaller PSD band is due to the loading of some larger pores with POM units that has caused narrowing of pore diameter, from 3.3 nm to 2.7 nm. It is believed that with successive loading of larger pores, some of the nearest larger pores could get distorted due to strong electrostatic interactions in the loaded pores. It is probable that such a distortion may have altered the pore dimensions of these few pores, from 3.0 nm to 3.3 nm.

3.2. Stability of monovacant POMs in the presence of H_2O_2

The study of the stability of monovacant TBAPW₁₁ and TBASiW₁₁ in presence of excess of H_2O_2 and MeCN/ H_2O mixtures was performed by electronic absorption spectroscopy and ³¹P NMR (for TBAPW₁₁). Keggin-type POMs show a characteristic UV band attributed to the charge transfer band from the oxygen to the tungsten. UV–vis and ³¹P NMR studies were performed for the ratios $[H_2O_2]/[XW_{11}]$ of 300 (20 μ mol of XW_{11} and 6 mmol H_2O_2) and 1500 (20 μ mol of XW_{11} and 30 mmol H_2O_2) mixtures at room temperature. The $[H_2O_2]/[XW_{11}] = 300$ corresponds to the excess of oxidant to the catalyst used in this work for the oxidation of cis-cyclooctene and the $[H_2O_2]/[XW_{11}] = 1500$ is the ratio used for the oxidation of geraniol and R-(+)-limonene. The study by UV–vis spectroscopy suggests that the monovacant TBASiW₁₁ seems to be stable or at least no appreciable decomposition was noticed for $[H_2O_2]/[SiW_{11}] = 300$ and 1500 since no significant variation of UV spectra (not shown) was observed ($\lambda_{max} = 258$ nm). Contrasting, it was noticed that TBAPW₁₁ was not stable in the

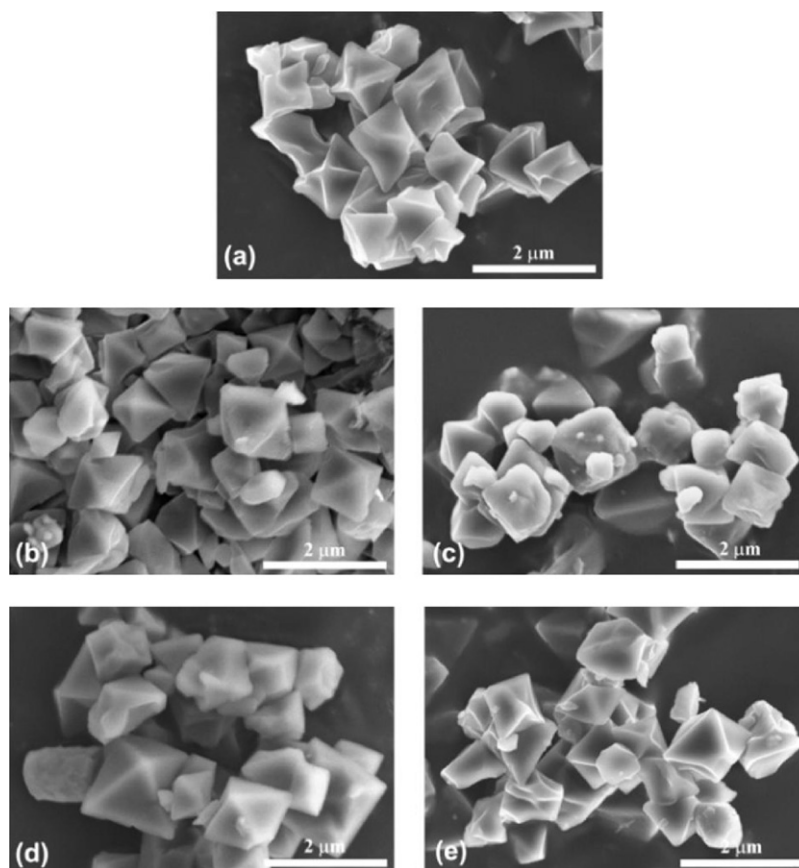


Fig. 5. SEM images of (a) MIL-101(Cr), (b) PW₁₁@MIL-101, (c) PW₁₁@MIL-101-ac, (d) SiW₁₁@MIL-101 and (e) SiW₁₁@MIL-101-ac (ac = after catalysis).

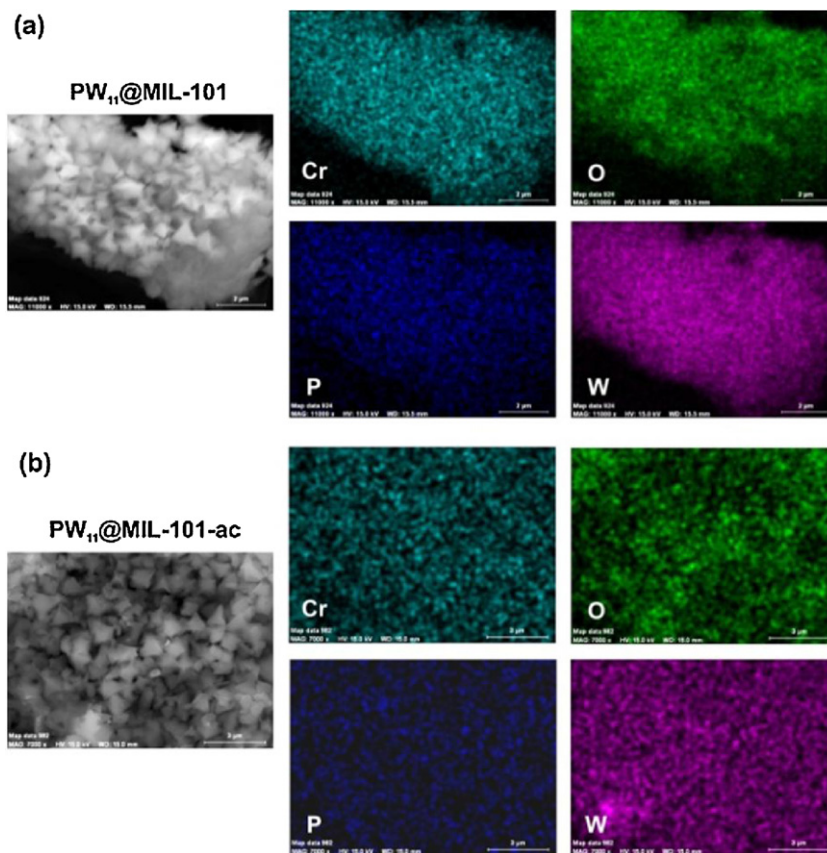


Fig. 6. EDX elemental mapping images for the composite material PW₁₁@MIL-101 and PW₁₁@MIL-101-ac (ac = after catalysis).

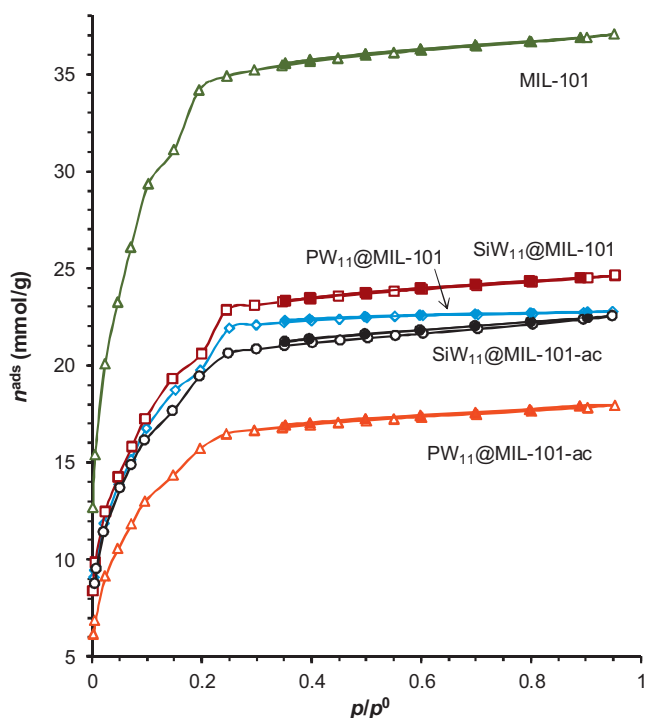


Fig. 7. The nitrogen adsorption–desorption isotherms of the studied materials at -196°C : MIL-101(Cr) (green), PW_{11} @MIL-101 (blue), PW_{11} @MIL-101-ac (red), SiW_{11} @MIL-101 (brown) and SiW_{11} @MIL-101-ac (black) (ac=after catalysis); unfilled and filled symbols represent the adsorption and desorption processes, respectively. (For interpretation of the references to colour in this figure legend, the reader is referred to the web version of this article.)

presence of H_2O_2 , in both ratios $[\text{H}_2\text{O}_2]/[\text{PW}_{11}]$ of 300 and 1500. The UV–vis spectra were collected at different times and was observed the decrease of the absorbance for the band with $\lambda_{\text{max}} = 255 \text{ nm}$ (see Fig. S7 of the Supporting Information). The decomposition of PW_{11} was faster in the presence of higher excess of H_2O_2 . Identical study was also performed by ^{31}P NMR for the same $[\text{H}_2\text{O}_2]/[\text{PW}_{11}]$ ratios (see Fig. S8 of the Supporting Information). A single peak attributed to PW_{11} was observed at -11.8 ppm until 30 min after the addition of H_2O_2 (see Supporting Information, Fig. S8a and S8b). However, after 1 h the PW_{11} was completely decomposed and other two peaks attributed to the products of decomposition were found at 0.8 and 3.2 ppm (see Fig. S8c of the Supporting Information). On the other hand, a similar experiment was performed with H_2O replacing H_2O_2 under identical condition (in particular $[\text{H}_2\text{O}_2]/[\text{PW}_{11}] = 1500$), however the decomposition of PW_{11} was not observed.

The decomposition of the Keggin anion PW_{12} in several peroxy-complexes in aqueous solution with H_2O_2 is well known since the beginning of the 90 decade [61,62]. Some years later, Griffith et al. reported the stability of PW_{11} in the presence of H_2O_2 in aqueous solution. In this case also the monovacant POM split up to a variety of peroxy-complexes, such as $[(\text{PO}_4)(\text{WO}(\text{O}_2)_2)_2]^{3-}$, $[(\text{PO}_4)(\text{WO}(\text{O}_2)_2)_2(\text{WO}(\text{O}_2)_2(\text{H}_2\text{O}))]^{3-}$ and $[(\text{PO}_3(\text{OH}))(\text{WO}(\text{O}_2)_2)_2]^{2-}$, some previously observed from PW_{12} decomposition [63]. In the same study the peroxy-complexes were characterized by ^{31}P NMR, revealing chemical shift near 3.0 ppm. More recently, it was described that the PW_{11} decomposes into Venturello complex $[(\text{PO}_4)(\text{WO}(\text{O}_2)_2)_4]^{3-}$ in the presence of H_2O_2 under a biphasic catalytic system, and the peak characteristic of this complex appears at 0.6 ppm [64]. In fact, this Venturello complex is probably one of the products of PW_{11} decomposition we observed in the presence of H_2O_2 excess and MeCN solution (see Fig. S8c of the Supporting Information).

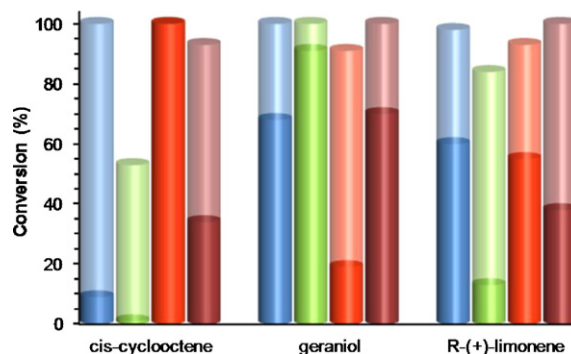


Fig. 8. Conversion obtained for the oxidation of cis-cyclooctene (ratio $[\text{H}_2\text{O}_2]/[\text{cis-cyclooctene}] = 1$, $T = 75^{\circ}\text{C}$), geraniol (ratio $[\text{H}_2\text{O}_2]/[\text{geraniol}] = 4.5$, room temperature) and R-(+)-limonene (ratio $[\text{H}_2\text{O}_2]/[\text{R-(+)-limonene}] = 4.5$, $T = 75^{\circ}\text{C}$) using the PW_{11} (blue), SiW_{11} (green) and the composite materials PW_{11} @MIL-101 (orange) and SiW_{11} @MIL-101 (dark red) as catalysts. The entire bars correspond to the conversion after 6 h of reaction, while the darker part of each bar represents only the conversion after 30 min. (For interpretation of the references to colour in this figure legend, the reader is referred to the web version of this article.)

3.3. Catalytic studies

The oxidation of cis-cyclooctene (i), geraniol (iii) and R-(+)-limonene (v) (Scheme 1) was carried out in homogeneous phase using TBA salts of the monovacant polyoxotungstates (TBAPW₁₁ and TBASiW₁₁). In the heterogeneous phase the composite materials PW_{11} @MIL-101 and SiW_{11} @MIL-101 were tested as catalysts, in the presence of H_2O_2 and MeCN as solvent. The catalytic activity of the support MIL-101(Cr) was investigated for the oxidation of the three selected substrates and the conversion was negligible, even after 24 h of reaction. Additionally, in the absence of catalyst using similar conditions to that of the catalytic reactions no conversion was verified.

The three distinct substrates were chosen to evaluate the catalytic efficiency of the homogeneous monovacant POMs, as well as their performance and robustness when incorporated in the MIL-101(Cr) cavities, for the oxidation reactions in a system combining H_2O_2 -MeCN as oxidant-solvent. Considerable differences were found for the conversion of the substrates and the distribution of oxidation products for the homogeneous and heterogeneous systems. Fig. 8 shows the conversion data for the oxidation of the selected substrates utilizing the homogeneous monovacant POMs (PW_{11} and SiW_{11}) and their composite materials (PW_{11} @MIL-101 and SiW_{11} @MIL-101) as catalysts.

Cis-cyclooctene. The oxidation of cis-cyclooctene (i, Scheme 1) was studied using equivalent amounts of oxidant and substrate. In the presence of all catalysts only 1,2-epoxycyclooctane (ii, Scheme 1) was formed. Interestingly, the heterogeneous catalysts PW_{11} @MIL-101 and SiW_{11} @MIL-101 revealed to be more active than the corresponding homogeneous monovacant polyanions (PW_{11} and SiW_{11}). In fact, with the heterogeneous catalyst PW_{11} @MIL-101 the conversion of cis-cyclooctene into 1,2-epoxycyclooctane was practically complete after 10 min of reaction (yield of 98% and TOF of $1922 \text{ mol mol}_{\text{POM}}^{-1} \text{ h}^{-1}$). Using an equivalent amount of homogeneous catalyst PW_{11} the conversion of cis-cyclooctene after 10 min was basically inexistent, however after 5 h of reaction the yield of 1,2-epoxycyclooctane attain 96%.

The phosphotungstate catalysts PW_{11} and PW_{11} @MIL-101 seemed to be more active than the analogues silicotungstates. This behaviour has been observed previously for other oxidative reactions and may be consequence of the weaker interactions between H_2O_2 and silicotungstates than with phosphotungstates [23]. In the presence of SiW_{11} @MIL-101 the almost complete epoxidation was only achieved after 6 h (93% of yield) and in the presence of

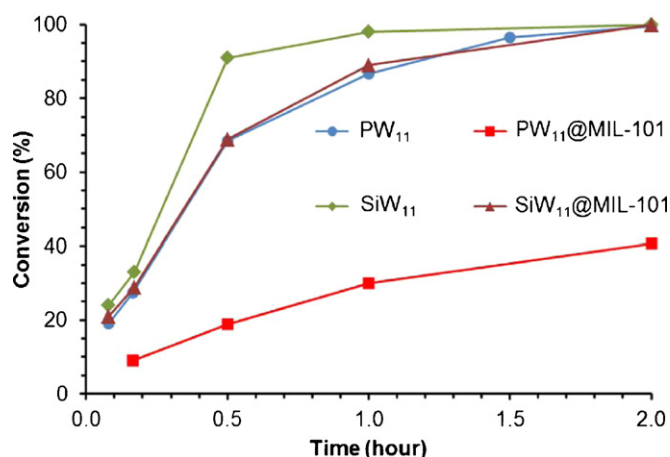


Fig. 9. Conversion data obtained for the oxidation of geraniol (ratio $[H_2O_2]/[geraniol]=4.5$, room temperature) using the PW_{11} (blue), SiW_{11} (green) in homogeneous phase, and the composite materials $PW_{11}@MIL-101$ (red) and $SiW_{11}@MIL-101$ (dark red) in heterogeneous phase.

the homogeneous SiW_{11} catalyst only 53% of conversion of cis-cyclooctene was attained. These results show that the inclusion of the active centres PW_{11} and SiW_{11} seems to improve the catalytic performance of these catalysts. This phenomenon may be caused by concentration effects promoted by adsorption of reactants in the cages of MIL-101(Cr). In fact, the mechanism proposed in the literature for alkenes epoxidation involves the formation of a hydroperoxy species ($POM-OOH$) as active intermediate, formed by the interaction of POM and H_2O_2 [65]. The epoxide is then formed by transferring an oxygen atom from the cleaved O–O bond of the $POM-OOH$ species. The effect of the porous cage where catalysts, oxidant and substrate are confined probably promotes a faster formation of the hydroperoxide active species and consequently the higher production of epoxide in shorter reaction time, when compared with the homogeneous system.

Geraniol. The oxidation of geraniol (iii, Scheme 1) can occur in different possible groups of this allylic alcohol, such as in the two double bonds, in the allylic carbon centres and in the carbon of the CH_2OH group. The oxidation of this substrate was performed at room temperature with light protection and using an excess of oxidant H_2O_2 relatively to the substrate. In the presence of both the homogeneous and heterogeneous catalysts only 2,3-epoxygeraniol (iv, Scheme 1) was obtained as product, demonstrating the high chemio-selectivity nature of the studied systems. Fig. 9 depicts the kinetic profile for the oxidation of geraniol catalyzed by the homogeneous and heterogeneous monovacant catalysts. The silicotungstates SiW_{11} and $SiW_{11}@MIL-101$ showed to be more active than the respective phosphotungstates PW_{11} and $PW_{11}@MIL-101$. The kinetic profile of SiW_{11} and $SiW_{11}@MIL-101$ is similar and the conversion of geraniol into 2,3-epoxydegeraniol was almost total after 1 h of reaction. The catalytic activity of $PW_{11}@MIL-101$ is considerably lower than the corresponding homogeneous catalyst PW_{11} . The turnover frequency calculated after 5 min of reaction for $PW_{11}@MIL-101$ is lower than the homogeneous PW_{11} and the silicotungstates SiW_{11} and $SiW_{11}@MIL-101$ (Table 2). The oxidation of this allylic alcohol involves coordination of the alcohol to the POM and the formation of a peroxo group adjacent to this site [66]. Thus, the essential coordination of the substrate to the catalyst occurred differently for PW_{11} and SiW_{11} , and this fact may be the main reason for the difference of activity observed.

In a recent investigation, our group studied the catalytic performance of the monovacant PW_{11} immobilized onto functionalized SBA-15 support ($PW_{11}@aptesSBA-15$) for the oxidation of geraniol. The catalytic activity of the material also was much

Table 2

Data from the oxidation of geraniol after 1 h of reaction, for different catalysts investigated^a.

Catalyst	Conversion (%)	TOF ^b (mol mol _{cat} ⁻¹ h ⁻¹)	Selectivity ^c (%)
No catalyst	≈0	–	–
PW_{11}	87	791	100
$PW_{11}@MIL-101$	30 (91) ^d	179	100
SiW_{11}	98	1000	100
$SiW_{11}@MIL-101$	89	875	100

^a Reaction conditions: 1 mmol of geraniol, 4.5 mmol H_2O_2 , 3 μ mol of POM or 42 or 46 mg of composite materials that contain 3 μ mol of POM , room temperature, light protection.

^b $TOF = (\text{moles of geraniol consumed}) / ((\text{moles of } POM) \times 0.08 \text{ h})$.

^c Based on the amount of consumed substrate, corresponding to 2,3-epoxygeraniol.

^d Conversion data obtained after 6 h of reaction.

lower than its homogeneous PW_{11} [36]. However, when the catalytic performance of the two different composites $PW_{11}@MIL-101$ and $PW_{11}@aptesSBA-15$ is compared it is noticed that the PW_{11} immobilized into MIL-101(Cr) is more active than the same immobilized onto aptesSBA-15. After 4 h of reaction the yield of 2,3-epoxygeraniol was 81% when the reaction was catalyzed by $PW_{11}@MIL-101$, instead of 50% obtained in the presence of $PW_{11}@aptesSBA-15$ [36]. The catalytic results obtained with the monovacant MIL-101(Cr) composites were also compared with other heterogeneous catalytic systems for the oxidation of geraniol using H_2O_2 as oxidant [67–71]. Higher conversion data were obtained in shorter reaction time and equivalent or even higher selectivity was achieved in the presence of $PW_{11}@MIL-101$ and $SiW_{11}@MIL-101$ catalysts.

R-(+)-limonene. The oxidation of R-(+)-limonene (v, Scheme 1) was also investigated in the presence of selected catalysts. The kinetic profile of PW_{11} and $PW_{11}@MIL-101$ is very similar and the oxidation of the substrate was almost complete after 3 h (Fig. 10). The turnover frequency obtained in the presence of the homogeneous PW_{11} and the heterogeneous $PW_{11}@MIL-101$ was 869 and 828 mol mol_{POM}⁻¹ h⁻¹, respectively. Identical amounts of limonene-1,2-epoxide (vi, Scheme 1) and limonene-1,2-diol (viii, Scheme 1) were obtained in the oxidation of R-(+)-limonene in the presence of the PW_{11} homogeneous and respective heterogeneous catalysts. However, small amounts of diepoxide (vii, Scheme 1) were also formed. The $SiW_{11}@MIL-101$ composite material also showed considerable activity in the oxidation of this monoterpene, since the conversion achieved after 3 h of reaction was

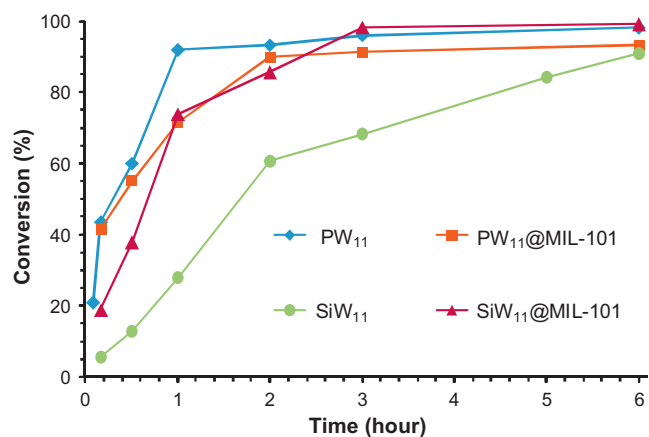


Fig. 10. Conversion attained for the oxidation of R-(+)-limonene (ratio $[H_2O_2]/[R-(+)-limonene]=4.5$, $T=75^\circ C$) using PW_{11} (blue), SiW_{11} (green) as homogeneous catalysts and the composite materials $PW_{11}@MIL-101$ (red) and $SiW_{11}@MIL-101$ (dark red) as heterogeneous catalysts.

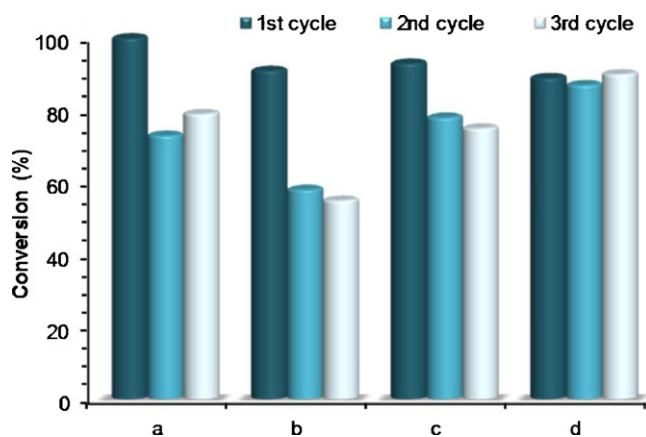


Fig. 11. Conversion data obtained for three consecutive cycles for the oxidation of cis-cyclooctene (ratio $[H_2O_2]/[cis-cyclooctene]=1$, $T=75^\circ C$) and geraniol (ratio $[H_2O_2]/[geraniol]=4.5$, at room temperature) using the composite materials PW₁₁@MIL-101 and SiW₁₁@MIL-101: (a) PW₁₁@MIL-101/cis-cyclooctene after 30 min, (b) PW₁₁@MIL-101/geraniol after 6 h, (c) SiW₁₁@MIL-101/cis-cyclooctene after 6 h and (d) SiW₁₁@MIL-101/geraniol after 30 min.

approximately complete (Fig. 10). On the other hand, the homogeneous SiW₁₁ showed to be slightly less active than its composite SiW₁₁@MIL-101. As described previously, this fact can be associated with the confinement effect produced by the MIL-101(Cr) cavities.

The literature reports only two examples of heterogeneous catalysts based in Keggin type POMs evaluated in the oxidation of limonene. One corresponds to a silicotungstate immobilized onto surface-modified SiO₂, which yield 78% of limonene-8,9-epoxide after 24 h of reaction [30]. The other example, was reported by our group, and corresponds to the monovacant PW₁₁ immobilized onto aptesSBA-15 [36]. In this case, the activity was lower than the corresponding homogeneous PW₁₁ and was necessary 24 h of reaction to approximate of the complete conversion. Therefore, we can conclude that the heterogeneous catalyst PW₁₁@MIL-101 is more active than the related PW₁₁@aptesSBA-15 material. Superior conversion data for shorter reaction time is also found comparing the catalytic performance of the monovacant MIL-101(Cr) composites with other silica or titanium heterogeneous catalysts using H₂O₂ as oxidant [72–74]. However, some of these studies present higher selectivity data for the epoxide of limonene [72,74].

The similarity of catalytic activity of homogeneous and heterogeneous promoted by the MIL-101(Cr) support should be associated with the morphology of its large cages, probably allowing some mobility to the POM inside the cavities.

3.4. Recyclability and leaching

The recyclability of the solid catalysts was studied for the oxidation reactions of cis-cyclooctene and geraniol. The catalysts were recovered from the reaction mixture by centrifugation, washed several times with MeCN and dried at room temperature to be used in a fresh reaction under identical experimental conditions (using the same ratio of catalyst: substrate: oxidant: solvent). Fig. 11 shows the reusability of the composites for the oxidation of both substrates with hydrogen peroxide. In general, the activity of PW₁₁@MIL-101 and SiW₁₁@MIL-101 in the oxidation of cis-cyclooctene and geraniol slightly decreases from the first to the second reaction cycle during the first hours of reaction. However after 24 h of reaction the conversion data is the same in all reaction cycles corresponding to the complete conversion of substrate. From the second to the third reaction cycle the activity of the catalysts is retained. This behaviour may indicate that some leaching of the

active species (PW₁₁ or SiW₁₁) of the catalyst should occur during the first reaction cycle.

To investigate the level of heterogeneity of the heterogeneous catalysts, leaching tests were performed to analyze the presence of active catalytic species in solution. Thus, the solid catalyst was separated from the reaction mixture by careful filtration after certain time and the reaction was further continued with the remaining filtrate. This experiment was performed for the oxidation of cis-cyclooctene using SiW₁₁@MIL-101, and for the oxidation of geraniol using PW₁₁@MIL-101. In the leaching test of SiW₁₁ based material for the oxidation of cis-cyclooctene, the solid catalyst was removed after 10 min of reaction. After this point the conversion of the substrate into its epoxide practically stopped, and even after 24 h of reaction the conversion only increased 15%. The results of the leaching analysis of PW₁₁@MIL-101 for geraniol oxidation were similar. The catalyst was removed after 1 h of reaction, and the conversion practically remained unaltered (even after 24 h the conversion only increased 17%). These results indicate that the materials are in fact heterogeneous and the loss of active monovacant species to the solutions is not significant.

To evaluate the possible loss of the POM anions from the composite materials to the solution, the W analysis of the recovered materials after the three consecutive reaction cycles was performed. From the initial loading of SiW₁₁ in SiW₁₁@MIL-101 only 10% was leached after three consecutive cycles (0.065 mmol of SiW₁₁ was found). For PW₁₁@MIL-101, the leaching of PW₁₁ species was higher, and 17% of the initial loading was lost for the solution during the reaction cycles (0.048 mmol of PW₁₁ was found in PW₁₁@MIL-101).

3.5. Catalyst materials stability and H₂O₂ efficiency

The structural stability of composite materials PW₁₁@MIL-101 and SiW₁₁@MIL-101 used as heterogeneous catalysts was investigated by several methods. In practice, after the three catalytic cycles the materials PW₁₁@MIL-101-ac and SiW₁₁@MIL-101-ac (where ac stands for after catalysis) were recovered and investigated by powder XRD, FT-IR and FT-Raman spectroscopies, ³¹P HPDEC NMR spectroscopy (only for the PW₁₁ based material), SEM, EDX and textural analysis.

The powder XRD patterns of the two heterogeneous catalysts performed in samples used in catalytic reaction are identical to the respective diffractogram before catalytic use, confirming the integrity of the crystalline structure of the solid support MIL-101(Cr) after various catalytic reaction cycles (see Fig. 4 for PW₁₁@MIL-101 and Fig. S3 of the Supporting Information for SiW₁₁@MIL-101). The maintenance of the structure was further recognized by electronic microscopy, SEM and EDX. As depicted in Fig. 5, the morphology of the PW₁₁@MIL-101-ac and SiW₁₁@MIL-101-ac is similar to that of the respective samples before catalysis. Additionally, the EDX spectra (not shown) and the EDX mapping confirm the existence of P and W, or Si and W in the composite materials after catalysis, and consequently points to the preservation of polyoxotungstates in the composite materials even after several subsequent catalytic cycles (see Fig. 6 and Fig. S5 of the Supporting Information for the PW₁₁ and SiW₁₁ based materials, respectively).

The retention of the polyoxotungstates in the MIL-101(Cr) framework after catalysis was also verified by FT-IR and FT-Raman spectroscopic studies. The comparison with the vibrational spectra of the as-synthesized materials (Figs. 1 and 2 for the PW₁₁ based material, and Fig. S2 of the Supporting Information for the SiW₁₁ based material) doesn't reveal significant changes on the typical bands of the MOF as well as in the observable vibrational modes of the POMs.

The nitrogen adsorption–desorption isotherms of $PW_{11}@MIL-101-ac$ and $SiW_{11}@MIL-101-ac$ are shown in Fig. 7. After catalysis the total pore volume of $PW_{11}@MIL-101$ gets reduced by ca. 21%, however this reduction is only ca. 8% for $SiW_{11}@MIL-101$. Comparing the relative decrease in V_{total} and V_{μ} after catalysis, it shows that these decreases are primarily due to decrease in V_{μ} , it points towards possibility of blocking in some of the loaded pores during catalysis. The PSD again gets changed, after catalysis, and returns to its previous stage, see Fig. S6 of the Supporting Information. It indicates that the loaded pores of $PW_{11}@MIL-101-ac$ and $SiW_{11}@MIL-101-ac$ might be partially stuffed/exhausted and are therefore inaccessible for N_2 adsorption. As a result, the PSD in this case is evolved mainly from non-loaded pores that remained as such after loading procedure.

The ^{31}P HPDEC MAS NMR spectrum of the composite $PW_{11}@MIL-101$ was performed after catalytic use (Fig. 3). Two peaks are observed at -15.72 and -13.51 ppm. To investigate the species corresponding to these peaks, the ^{31}P HPDEC MAS NMR spectrum of the composite $PW_{12}@MIL-101$ was performed and a single peak was found at -15.92 ppm (Fig. 3). Thus, one of the two peaks observed for the spectrum of $PW_{11}@MIL-101$ may indicate a small decomposition of PW_{11} into PW_{12} inside of MIL-101(Cr) cage. The other peak may be attributed to PW_{11} with a saturation in its lacunary region with other species (such as the oxidant and/or solvent), originating a shift from -10.65 to -13.51 ppm, as observed before in the literature for PW_{11} immobilized into silica nanoparticles [35,57]. However, the transformation of PW_{11} into peroxy compounds when excess of H_2O_2 is present was not observed when the composite $PW_{11}@MIL-101$ was exposed to the same excess of H_2O_2 . These results suggest that the MIL-101(Cr) can confer some stability to the PW_{11} structure without changing its catalytic activity.

The combination of the evidences from the wide range of characterization methods used to characterize the materials after catalytic use (after three reaction cycles), $PW_{11}@MIL-101-ac$ and $SiW_{11}@MIL-101-ac$, strongly suggests that the materials investigated are reasonable robust and stable heterogeneous catalysts.

The efficiency of usage of H_2O_2 was determined for the oxidation of different studied substrates. For the oxidation of cis-cyclooctene and geraniol the efficiency of oxidant was similar in the presence of $PW_{11}@MIL-101$ and $SiW_{11}@MIL-101$ catalysts. For both substrates 100% of selectivity for the corresponding epoxide was obtained and an efficiency of H_2O_2 near 100% and 95% was found for the oxidation of cis-cyclooctene and geraniol, respectively. The efficiency of H_2O_2 decreases for the oxidation of R-(+)-limonene when three different products (epoxide, diol and diepoxide) were obtained. In this case, the efficiency of H_2O_2 was higher in the presence of $PW_{11}@MIL-101$ (43%) than in the presence of $SiW_{11}@MIL-101$ (60%), even though the product spectrum was similar.

4. Conclusions

The monovacant PW_{11} and SiW_{11} anions were immobilized into MIL-101(Cr) framework, forming hybrid composite materials, $PW_{11}@MIL-101$ and $SiW_{11}@MIL-101$ respectively, which revealed retention of POMs and MOF structures. The incorporation of the two POMs in the MIL-101(Cr) cavities was unequivocally confirmed by the combination of a vast number of complementary characterization methods such as, powder XRD, FT-IR and FT-Raman spectroscopy, ^{31}P solid-state NMR spectroscopy (only for the PW_{11} based material), elemental analysis, scanning electron microscopy (SEM), energy-dispersive X-ray spectroscopy (EDX) and nitrogen adsorption–desorption isotherms. The poor stability of PW_{11} anion observed in homogeneous phase was enhanced when the same was incorporated into MIL-101(Cr). In this case, the structure of

MIL-101(Cr) showed to have a relevant influence in the PW_{11} stability in the presence of H_2O_2 . In the perspective view of achieving novel high performance catalytic systems, the composites $PW_{11}@MIL-101$ and $SiW_{11}@MIL-101$ were tested for the oxidation of cis-cyclooctene, geraniol and R-(+)-limonene, using H_2O_2 as oxidant. These composites showed to be active, robust and selective heterogeneous catalysts. $PW_{11}@MIL-101$ proved to be more efficient catalyst than the homogeneous PW_{11} for the epoxidation of cis-cyclooctene into 1,2-epoxycyclooctane (complete conversion after the first 10 min of reaction). Similar activity between homogeneous monovacant species and the composites were found for geraniol and R-(+)-limonene oxidation. From the first reaction a complete conversion into 2,3-epoxygeraniol was achieved after 1 h of reaction in the presence of $SiW_{11}@MIL-101$. From the R-(+)-limonene oxidation, complete conversion was enhanced after 3 h in the presence of $PW_{11}@MIL-101$. The integrity and robustness of both composites materials, $PW_{11}@MIL-101$ and $SiW_{11}@MIL-101$, were confirmed after catalytic uses by several techniques. Following the interesting results of the present work, we are currently investigating the use of other porous MOFs and distinct POMs to prepare novel catalysts for oxidation reactions.

Acknowledgments

The authors acknowledge the Fundação para a Ciência e a Tecnologia (FCT, MEC, Portugal) for their general financial support through the strategic projects Pest-C/EQB/LA0006/2011 (to Associated Laboratory REQUIMTE), Pest-OE/QUI/UI0612/2011 (to CQB) and Pest-C/CTM/LA0011/2011 (to the Associated Laboratory CICECO), the R&D projects PTDC/CTM/100357/2008 and PTDC/EQU-EQU/121677/2010, and the fellowships SFRH/BPD/73191/2010 (to CG) SFRH/BPD/77216/2011 (to VKS) and SFRH/BD/46601/2008 (to PS).

Appendix A. Supplementary data

Supplementary data associated with this article can be found, in the online version, at <http://dx.doi.org/10.1016/j.apcata.2012.12.039>.

References

- [1] C. Gucuyener, J. van den Bergh, J. Gascon, F. Kapteijn, J. Am. Chem. Soc. 132 (2010) 17704–17706.
- [2] R.B. Getman, Y.-S. Bae, C.E. Wilmer, R.Q. Snurr, Chem. Rev. 112 (2012) 703–723.
- [3] M.P. Suh, H.J. Park, T.K. Prasad, D.-W. Lim, Chem. Rev. 112 (2012) 782–835.
- [4] K. Sumida, D.L. Rogow, J.A. Mason, T.M. McDonald, E.D. Bloch, Z.R. Herm, T.-H. Bae, J.R. Long, Chem. Rev. 112 (2012) 724–781.
- [5] J.-R. Li, J. Sculley, H.-C. Zhou, Chem. Rev. 112 (2012) 869–932.
- [6] A. Corma, H. Garcia, F.X.L. Xamena, Chem. Rev. 110 (2010) 4606–4655.
- [7] M. Ranocchiari, J.A. van Bokhoven, Phys. Chem. Chem. Phys. 13 (2011) 6388–6396.
- [8] J. Lee, O.K. Farha, J. Roberts, K.A. Scheidt, S.T. Nguyen, J.T. Hupp, Chem. Soc. Rev. 38 (2009) 1450–1459.
- [9] M. Yoon, R. Srirambalaji, K. Kim, Chem. Rev. 112 (2012) 1196–1231.
- [10] A. Dhakshinamoorthy, M. Alvaro, H. Garcia, Catal. Sci. Technol. 1 (2011) 856–867.
- [11] D.Y. Hong, Y.K. Hwang, C. Serre, G. Ferey, J.S. Chang, Adv. Funct. Mater. 19 (2009) 1537–1552.
- [12] Z.Y. Gu, X.P. Yan, Angew. Chem. Int. Ed. 49 (2010) 1477–1480.
- [13] N.V. Maksimchuk, K.A. Kovalenko, S.S. Arzumanov, Y.A. Chesalov, M.S. Melgunov, A.G. Stepanov, V.P. Fedin, O.A. Kholdeeva, Inorg. Chem. 49 (2010) 2920–2930.
- [14] A. Sonnauer, F. Hoffmann, M. Froba, L. Kienle, V. Duppel, M. Thommes, C. Serre, G. Ferey, N. Stock, Angew. Chem. Int. Ed. 48 (2009) 3791–3794.
- [15] Y.K. Hwang, D.Y. Hong, J.S. Chang, H. Seo, M. Yoon, J. Kim, S.H. Jung, C. Serre, G. Ferey, Appl. Catal. A: Gen. 358 (2009) 249–253.
- [16] G. Ferey, C. Mellot-Draznieks, C. Serre, F. Millange, J. Dutour, S. Surble, I. Margiolaki, Science 309 (2005) 2040–2042.
- [17] M. Latroche, S. Surble, C. Serre, C. Mellot-Draznieks, P.L. Llewellyn, J.H. Lee, J.S. Chang, S.H. Jung, G. Ferey, Angew. Chem. Int. Ed. 45 (2006) 8227–8231.
- [18] O.I. Lebedev, F. Millange, C. Serre, G. Van Tendeloo, G. Ferey, Chem. Mater. 17 (2005) 6525–6527.

- [19] P. Horcajada, C. Serre, M. Vallet-Regi, M. Sebban, F. Taulelle, G. Férey, *Angew. Chem. Int. Ed.* 45 (2006) 5974–5978.
- [20] Y.B. Huang, Z.J. Lin, R. Cao, *Chem. Eur. J.* 17 (2011) 12706–12712.
- [21] C.L. Hill, *J. Mol. Catal. A Chem.* 262 (2007), 1–1.
- [22] N. Mizuno, K. Yamaguchi, K. Kamata, *Coord. Chem. Rev.* 249 (2005) 1944–1956.
- [23] M.S.S. Balula, I.C.M.S. Santos, M.M.Q. Simões, M.G.P.M.S. Neves, J.A.S. Cavaleiro, A.M.V. Cavaleiro, *J. Mol. Catal. A Chem.* 222 (2004) 159–165.
- [24] I.C.M.S. Santos, M.M.Q. Simões, M.S.S. Balula, M.G.P.M.S. Neves, J.A.S. Cavaleiro, A.M.V. Cavaleiro, *Synlett* (2008) 1623–1626.
- [25] C.L. Hill, C.M. Prosser, *Coord. Chem. Rev.* 143 (1995) 407–455.
- [26] Y. Kikukawa, K. Yamaguchi, N. Mizuno, *Angew. Chem. Int. Ed.* 49 (2010) 6096–6100.
- [27] M.M.Q. Simões, I.C.M.S. Santos, M.S.S. Balula, J.A.F. Gamelas, A.M.V. Cavaleiro, M.G.P.M.S. Neves, J.A.S. Cavaleiro, *Catal. Today* 91–2 (2004) 211–214.
- [28] M.M.Q. Simões, C.M.M. Conceicao, J.A.F. Gamelas, P. Domingues, A.M.V. Cavaleiro, J.A.S. Cavaleiro, A.J.V. Ferrer-Correia, R.A.W. Johnstone, *J. Mol. Catal. A Chem.* 144 (1999) 461–468.
- [29] A.C. Estrada, I.C.M.S. Santos, M.M.Q. Simões, M.G.P.M.S. Neves, J.A.S. Cavaleiro, A.M.V. Cavaleiro, *Appl. Catal. A: Gen.* 392 (2011) 28–35.
- [30] J. Kasai, Y. Nakagawa, S. Uchida, K. Yamaguchi, N. Mizuno, *Chem. Eur. J.* 12 (2006) 4176–4184.
- [31] O.A. Kholdeeva, N.V. Maksimchuk, G.M. Maksimov, *Catal. Today* 157 (2010) 107–113.
- [32] S.K. Jana, Y. Kubota, T. Tatsumi, *J. Catal.* 255 (2008) 40–47.
- [33] P.A. Shringarpure, A. Patel, *Dalton Trans.* 39 (2010) 2615–2621.
- [34] R.F. Zhang, C. Yang, *J. Mater. Chem.* 18 (2008) 2691–2703.
- [35] Y.H. Guo, Y. Yang, C.W. Hu, C.X. Guo, E.B. Wang, Y.C. Zou, S.H. Feng, *J. Mater. Chem.* 12 (2002) 3046–3052.
- [36] S.S. Balula, I.C.M.S. Santos, L. Cunha-Silva, A.P. Carvalho, J. Pires, C. Freire, J.A.S. Cavaleiro, B. de Castro, A.M.V. Cavaleiro, *Catal. Today*, <http://dx.doi.org/10.1016/j.cattod.2012.02.020>, in press.
- [37] N.V. Maksimchuk, M.N. Timofeeva, M.S. Melgunov, A.N. Shmakov, Y.A. Chesalov, D.N. Dybtsev, V.P. Fedin, O.A. Kholdeeva, *J. Catal.* 257 (2008) 315–323.
- [38] N.V. Maksimchuk, O.A. Kholdeeva, K.A. Kovalenko, V.P. Fedin, *Isr. J. Chem.* 51 (2011) 281–289.
- [39] J. Juan-Alcaniz, E.V. Ramos-Fernandez, U. Lafont, J. Gascon, F. Kapteijn, *J. Catal.* 269 (2010) 229–241.
- [40] E.V. Ramos-Fernandez, C. Pieters, B. van der Linden, J. Juan-Alcaniz, P. Serra-Crespo, M. Verhoeven, H. Niemantsverdriet, J. Gascon, F. Kapteijn, *J. Catal.* 289 (2012) 42–52.
- [41] L.H. Wee, S.R. Bajpe, N. Janssens, I. Hermans, K. Houthoofd, C.E.A. Kirschhock, J.A. Martens, *Chem. Commun.* 46 (2010) 8186–8188.
- [42] L.H. Wee, N. Janssens, S.R. Bajpe, C.E.A. Kirschhock, J.A. Martens, *Catal. Today* 171 (2011) 275–280.
- [43] C.-Y. Sun, S.-X. Liu, D.-D. Liang, K.-Z. Shao, Y.-H. Ren, Z.-M. Su, *J. Am. Chem. Soc.* 131 (2009) 1883–1888.
- [44] G. Hundal, Y.K. Hwang, J.-S. Chang, *Polyhedron* 28 (2009) 2450–2458.
- [45] Z.X. Zhang, W. Zhao, B.C. Ma, Y. Ding, *Catal. Commun.* 12 (2010) 318–322.
- [46] X.J. Luo, C. Yang, *Phys. Chem. Phys.* 13 (2011) 7892–7902.
- [47] P. Shringarpure, A. Patel, *Dalton Trans.* (2008) 3953–3955.
- [48] M.S. Balula, J.A. Gamelas, H.M. Carapuça, A.M.V. Cavaleiro, W. Schlindwein, *Eur. J. Inorg. Chem.* (2004) 619–628.
- [49] A. Tézé, G. Hervé, *Inorg. Synth* 27 (1992) 89.
- [50] C. Brevard, R. Schimpf, G. Tourne, C.M. Tourne, *J. Am. Chem. Soc.* 105 (1983) 7059–7063.
- [51] R.R.L. Martins, M.G.P.M.S. Neves, A.J.D. Silvestre, A.M.S. Silva, J.A.S. Cavaleiro, *J. Mol. Catal. A: Chem.* 137 (1999) 41–47.
- [52] R.R.L. Martins, M.G.P.M.S. Neves, A.J.D. Silvestre, M.M.Q. Simões, A.M.S. Silva, A.C. Tomé, J.A.S. Cavaleiro, P. Tagliatesta, C. Crestini, *J. Mol. Catal. A Chem.* 172 (2001) 33–42.
- [53] A.I. Vogel, *A Text-Book of Quantitative Inorganic Analysis Including Elementary Instrumental Analysis*, 3rd ed., Longmans, London, 1961.
- [54] C. Rocchicciolideltcheff, M. Fournier, R. Franck, R. Thouvenot, *Inorg. Chem.* 22 (1983) 207–216.
- [55] R. Massart, R. Contant, J.M. Fruchart, J.P. Ciabrini, M. Fournier, *Inorg. Chem.* 16 (1977) 2916–2921.
- [56] L.R. Pizzio, C.V. Caceres, M.N. Blanco, *Appl. Surf. Sci.* 151 (1999) 91–101.
- [57] Y. Yang, Y.H. Guo, C.W. Hu, C.J. Jiang, E.B. Wang, *J. Mater. Chem.* 13 (2003) 1686–1694.
- [58] K.S.W. Sing, D.H. Everett, R.A.W. Haul, L. Moscou, R.A. Pierotti, J. Rouquerol, T. Siemieniowska, *Pure Appl. Chem.* 57 (1985) 603–619.
- [59] P.L. Llewellyn, S. Bourrelly, C. Serre, A. Vimont, M. Daturi, L. Hamon, G. De Weireld, J.S. Chang, D.Y. Hong, Y.K. Hwang, S.H. Jhung, G. Férey, *Langmuir* 24 (2008) 7245–7250.
- [60] Y. Tajima, *Biol. Pharmacol. Bull.* 24 (2001) 1079–1084.
- [61] C. Aubry, G. Chottard, N. Platzter, J.M. Bregeault, R. Thouvenot, F. Chauveau, C. Huet, H. Ledon, *Inorg. Chem.* 30 (1991) 4409–4415.
- [62] L. Salles, C. Aubry, R. Thouvenot, F. Robert, C. Doremieuxmorin, G. Chottard, H. Ledon, Y. Jeannin, J.M. Bregeault, *Inorg. Chem.* 33 (1994) 871–878.
- [63] N.M. Gresley, W.P. Griffith, A.C. Laemmel, H.I.S. Nogueira, B.C. Parkin, *J. Mol. Catal. A-Chem.* 117 (1997) 185–198.
- [64] Z.H. Weng, J.Y. Wang, X.G. Jian, *Catal. Commun.* 9 (2008) 1688–1691.
- [65] R. Prabhakar, K. Morokuma, C.L. Hill, D.G. Musaev, *Inorg. Chem.* 45 (2006) 5703–5709.
- [66] A.J. Stapleton, M.E. Sloan, N.J. Napper, R.C. Burns, *Dalton Trans.* (2009) 9603–9615.
- [67] L.J. Schofield, O.J. Kerton, P. McMorn, D. Bethell, S. Ellwood, G.J. Hutchings, *J. Chem. Soc., Perkin Trans. 2* (2002) 1475–1481.
- [68] F. Somma, G. Strukul, *J. Catal.* 227 (2004) 344–351.
- [69] F. Somma, A. Puppinato, G. Strukul, *Appl. Catal. A: Gen.* 309 (2006) 115–121.
- [70] A. Feliczak-Guzik, I. Nowak, *Catal. Today* 142 (2009) 288–292.
- [71] N. Marin-Astorga, J.J. Martinez, G. Borda, J. Cubillos, D.N. Suarez, H. Rojas, *Top. Catal.* 55 (2012) 620–624.
- [72] P.C. Bakala, E. Briot, L. Salles, J.M. Bregeault, *Appl. Catal. A: Gen.* 300 (2006) 91–99.
- [73] A.J. Bonon, D. Mandelli, O.A. Kholdeeva, M.V. Barmatova, Y.N. Kozlov, G.B. Shul'pin, *Appl. Catal. A: Gen.* 365 (2009) 96–104.
- [74] F. Carniato, C. Bisio, L. Sordelli, E. Gavrilova, M. Guidotti, *Inorg. Chim. Acta* 380 (2012) 244–251.